Int J Mech Mater Des (2024) 20:1209–1228
https://doi.org/10.1007/s10999-024-09722-8

Voxel-based evolutionary topological optimization of connected structures for natural frequency optimization

Antonio Bacciaglia · Alessandro Ceruti · Alfredo Liverani

Received: 16 May 2024 / Accepted: 15 July 2024 / Published online: 1 August 2024

Abstract The topology optimization methodology is widely utilized in industrial engineering for designing lightweight and efficient components. In this framework, considering natural frequencies is crucial for adequately designing components and structures exposed to dynamic loads, as in aerospace or automotive applications. The scientific community has shown the efficiency of Bi-directional Evolutionary Structural Optimization (BESO), showcasing its ability to converge towards optimal solid-void or bi-material solutions for a wide range of frequency optimization problems in continuum structures. However, these methods show limits when the complexity of the domain volume increases; thus, they are well-suited for academic case studies but may fail when dealing with industrial applications that require more complex shapes. The connectivity of the structures resulting from the optimization also plays a fundamental role in choosing the best optimization approach, as some available commercial and open-source codes nowadays return unfeasible sparse structures. An improved voxel-based BESO algorithm has been developed in this work to cope with current limits in lightweight structure optimization. A significant case study has been developed to evaluate the performances of the new methodology and compare it with existing algorithms. In contrast to previous studies, the method we developed guarantees that the final structure respects constraints on the initial design volume and that the structure's connection is preserved, thus enabling the manufacturing of the component with Additive Manufacturing technologies. The proposed approach can be complemented by smoothing algorithms to obtain a structure with externally appealing surfaces.

Keywords Topology optimization · Natural frequency · Bi-directional evolutionary structural optimization (BESO) · Optimal design · Additive manufacturing

A. Bacciaglia · A. Ceruti (✉) · A. Liverani
Department of Industrial Engineering (DIN), University of Bologna, Bologna, Italy
e-mail: alessandro.ceruti@unibo.it

A. Bacciaglia
e-mail: antonio.bacciaglia2@unibo.it

A. Liverani
e-mail: alfredo.liverani@unibo.it

1 Introduction

Topology optimization (TO) is a numerical design approach that enables the development of efficient and lightweight components (Sigmund and Maute 2013). This design methodology finds particular application in industries such as automotive (Freddi et al. 2023; Torigaki and Fujitani 2000) and aerospace (Oktay et al. 2014). Intensive research on lightweight structures is pursued to enhance performance, reduce manufacturing and maintenance costs, and lower

energy consumption and emissions. Indeed, the next generation of urban air vehicles based on electric propulsion needs efficient structures due to the higher mass-to-energy ratios of batteries compared to fossil fuels. A significant contribution from the scientific community to the research on lightweight structures (i.e. TO) could be the correct answer to the needs of the coming years. However, the intricate and complex geometrical solutions resulting from TO analyses pose challenges for direct manufacturing through traditional chip removal processes for 3D models.

Conversely, the complexity of the structures aligns well with Additive Manufacturing (AM) techniques, which involve layer-by-layer material deposition (Murr 2016). AM is recognized for its freedom of shaping, a short design-to-manufacturing cycle, the ability to manufacture intricate biomimetic shapes featuring high strength-to-weight ratios, and reduce the number of parts, thus minimizing the need for bolted connections or welding (Abdulhameed et al. 2019).

TO significantly influences the shape of the structures, obtaining complex topologies; NURBS is a precise geometric representation that can describe complex shapes in the context of topology optimization (Zhuang et al. 2023). Every iteration's boundary may be precisely described geometrically thanks to the NURBS formulation, which makes it simple to compute local values (such as curvature radius) using the NURBS formal technique (Ghasemi et al. 2015). However, sharp corners and asymmetrical shapes are examples of complex topologies that NURBS models have trouble representing. In these situations, precise control point manipulation is necessary to produce high-quality surfaces with G2 continuity. After optimization, industrial components often present shapes that NURBS modelling can hardly describe.

TO has been the subject of extensive research over the past few decades. A wide range of optimization approaches, such as the Solid Isotropic Material with Penalization (SIMP) method (Andreassen et al. 2011; Rietz 2001), the Evolutionary Structural Optimization (ESO) method (Xie and Steven 1996), the homogenization method (Noguchi and Yamada 2021) and the level set technique (Ghasemi et al. 2018) have been devised within this field. A critical review of those approaches can be found in (Rozvany 2009) to give the reader more details.

When considering the above-listed methods, the SIMP technique handles the material density of individual elements as the design variable, allowing for continuous variation from 0 (void) to 1 (solid). The optimization goal is to find the optimal distribution of material within a given design space to minimize compliance (or maximize the stiffness) while adhering to a fixed volume fraction constraint. Intermediate densities are artificially penalized using a proper objective function, steering the optimization solution toward either solid (black) or void (white) elements (Ferrari and Sigmund 2020).

On the other hand, the fundamental idea behind the ESO approach is the gradual removal of inefficient materials, allowing the structure's residual shape to evolve towards an optimum state. Its evolution, known as Bi-directional ESO (BESO), goes beyond material removal and introduces the capability to add material simultaneously (Xia et al. 2018). The original ESO/BESO methods work as purely heuristic approaches, seeking the best solution from many possibilities generated during optimization. Occasionally, results may seem nonsensical if the tuning parameters are not optimally configured (Han et al. 2021). However, by combining BESO with a soft interpolating material scheme restricted to 1 and x_{min} (where x_{min} indicates the density of an element and often assumes values lower than 10^{-6} to indicate void spaces) and coupled with stringent optimality criteria, the revised BESO algorithm yields convergent solutions for stiffness optimization problems (Huang and Xie 2009).

While stiffness optimization problems were widely discussed in the literature, publications dealing with frequency optimization are limited in number. However, this topic is of fundamental importance in industrial applications characterized by cyclic loads environments, e.g., aerospace (Langley and Bardell 1998) and automotive (Qatu et al. 2009). In those fields, resonance, power spectral density, and fatigue play such an important role that a component often bears loads well below the yielding stress, which should be considered the dimensioning requirement (Wu et al. 2020). Significant deformations or fractures may result from resonance, brought on by the external excitation frequency equal to or near the structure's natural frequency. In order to maintain a safe distance from operating frequencies, it is crucial to build structures with suitable natural frequencies to avoid resonance. Maximizing natural frequencies and

frequency gaps is the most popular and efficient way to accomplish the above objective (Zargham et al. 2016).

Previous studies demonstrated that a purely SIMP method needs to improve in frequency optimization, primarily due to the emergence of artificial localized modes in regions of lower mass (Pedersen 2000). Earlier research on frequency optimization using ESO/BESO methods is documented, showcasing how the original hardkill ESO/BESO techniques successfully avoid the occurrence of localized vibration modes. However, shortcomings of the aforementioned ESO/BESO methods persist in frequency optimization problems.

For this reason, Huang et al. developed a modified SIMP method with a minor adjustment by maintaining a consistent ratio between mass and stiffness for both solid and void elements (Huang et al. 2010). This modification aims to prevent the occurrence of artificial localized modes during frequency optimization. Moreover, a sensitivity analysis for a specific frequency is included in their study. The sensitivity numbers, indicating the relative ranking of elemental sensitivities, are established and used in the BESO method with discrete design variables set at 1 or x_{min}. The straightforward BESO update scheme, in conjunction with rigorous optimality criteria, is employed to explore the optimal design that meets the prescribed volume/weight constraint.

The method proposed by Huang et al. fits well with academic case studies since an entire initial design domain in the shape of a parallelepiped can be analyzed. However, the design domain of real-life components could be very complex due to assembly constraints or the presence of no design spaces. Moreover, the method developed by Huang et al. needs to include a routine that guarantees the connectivity of the optimized structures to avoid Artificial Localized Rigid Motion (ALRM) modes. When low-volume fractions are requested, standard frequency optimization algorithms may return a not-fully-connected component that cannot be manufactured. This issue is especially true when complex shapes, typical of industrial applications, are considered. Also, commercial optimization software packages suffer a similar limitation, which can be experienced when optimizing a complex component with a low volume fraction. The approach proposed by (Deng et al. 2024) provides a solution to ALRM modes during the optimization process by controlling the Betti's number B_0, defined as the number of independent connected components (Liang et al. 2022). Deng et al. provide a discrete variable topology optimization approach based on Sequential Approximate Integer Programming (SAIP, (Liang et al. 2020)) that embeds a control on Betti's number. Both 2D and 3D case studies show some promising outcomes; however, the technique has only been used on academic geometries, and the authors omit to mention the simulation time—a crucial factor in actual industrial case studies.

As far as the authors are aware, the examination of the state of the art indicates a technological gap in optimizing the topology of 3D complex (non-academic) geometries, incorporating a process to verify structure connection, with reduced simulation times.

Thus, this research proposes a voxel-based evolutionary topological optimization method based on voxelization to handle complex design spaces. Voxelization, as a graphical method, involves representing a three-dimensional object using voxels, which are volumetric pixels (Jense 1989). Each voxel corresponds to a discrete, regularly spaced element in a three-dimensional grid.

The proposed methodology's capabilities are enhanced by handling complex design spaces, including no design zones, and ensuring a fully connected structure. A similar method has already been used by (Smit et al. 2021): it is based on volume voxelization to identify the design domain and possible no-design spaces. However, Smit et al. minimize compliance problems based on the SIMP approach, which is not directly applicable to frequency optimization. Moreover, the authors did not include a proper routine to guarantee the final structure connectivity.

Our approach includes a preliminary voxelization phase of the real-life component to convert it into a logical 3D matrix corresponding to the initial design domain. Consequently, the optimization algorithm of Huang et al. can be applied to any initial geometry of whatever complexity. Then, a routine that controls the full connectivity of the optimized structure at each iteration, even for low-volume fraction requirements runs. In this paper, the algorithm implements the bwconncomp

MATLAB function. Such a routine ensures that the optimized structure is feasible and manufacturable. Alternative methods described in the literature could also be applied (Cohen-Or and Kaufman 1997). As the last contribution of this manuscript, a Graphic User Interface (GUI) in MATLAB has been programmed to correctly set the boundary conditions of the problem in terms of constrained points and eventual point masses, thus growing the possible set of boundary conditions of the optimization problem described by Huang et al., and meet design capabilities closer to real-world case studies.

The paper is organized as follows: Section 2 recaps the fundamental optimization problem for frequency, introducing the modified SIMP model with sensitivity numbers for solid and soft elements derived according to the conventional sensitivity analysis; it briefly illustrates the voxelization method implemented in this study and the effects of the integration of a connectivity check routine. Section 3 briefly illustrates the BESO procedure and its numerical implementation. Section 4 presents the numerical results from the proposed evolutionary method when applied to a complex case study and compares them with commercial software. Concluding remarks and guidelines for future improvement are included in Section 5.

2 Methodology

This research aims to establish a new evolutionary optimization strategy that might be used to design structural components in a cyclic load environment where specific design constraints on the natural frequencies may be of straightforward importance. The proposed approach combines the voxelization method to prepare the design volume domain, the modified BESO method proposed by (Huang et al. 2010), and a specific algorithm to guarantee the full connectivity of the resulting structure. This Section describes the fundamentals of the optimization problem for frequency with the modified SIMP model, the graphic voxelization method, and how the connectivity check routine works.

2.1 Evolutionary topological optimization for natural frequencies

The dynamic characteristics of a continuous structure can be expressed through the principal eigenvalue problem outlined in eq. 1:

$$\left(\boldsymbol{K}-\omega_i^2\boldsymbol{M}\right)\boldsymbol{u}_i=0 \tag{1}$$

Here, $\boldsymbol{K}$ denotes the global stiffness matrix, $\boldsymbol{M}$ stands for the global mass matrix, ω_i represents the i-th natural frequency, and $\boldsymbol{u}_i$ is the corresponding eigenvector to ω_i. The Rayleigh quotient relates these two last parameters (eq. 2).

$$\omega_i=\frac{\boldsymbol{u}_i^T\boldsymbol{K}\boldsymbol{u}_i}{\boldsymbol{u}_i^T\boldsymbol{M}\boldsymbol{u}_i} \tag{2}$$

This research addresses topology optimization to maximize the i-th natural frequency in vibrating continuum structures. Consequently, for a design involving both solid and void regions, the optimization problem can be formulated as presented in eq. 3.

$$\begin{cases} \max(\omega_i) \\ V_f=\sum_{i=1}^{N} V_i x_i \\ x_i = x_{min} or 1 \end{cases} \tag{3}$$

V_i represents the volume of a single element while V_f indicates the desired volume fraction after the optimization. N denotes the total count of elements within the structure. The binary design variable x_i indicates the density of the ith element; if a small value is assigned, such as x_{min} (e.g., 10^{-6}), it denotes a void element.

It is essential to interpolate the material between x_{min} and 1 using a material interpolation scheme to acquire gradient information for the design variable. The commonly used power-law penalization model, known as the SIMP model, cannot be directly employed in frequency optimization problems due to the emergence of artificial localized modes in low-density regions. Hence, an alternative method for material interpolation can be articulated as in eq. 4 (Huang et al. 2010), where the present model converges indefinitely toward the original SIMP model as x_{min} approaches zero.

$$\begin{cases} \rho(x_i) = x_i \rho^1 \\ E(x_i) = \left[\frac{x_{min} - x_{min}^p}{1 - x_{min}^p} \left(1 - x_i^p\right) + x_i^p \right] E^1 \; for \; 0 < x_{min} \leq x_i \leq 1 \end{cases} \tag{4}$$

Here ρ^1 and E^1 express the density and Young's modulus of the solid material. The elemental stiffness and mass matrices for solid elements ($\boldsymbol{K}_i^1$ and $\boldsymbol{M}_i^1$) can be obtained as derivatives of $\boldsymbol{K}$ and $\boldsymbol{M}$ with respect to the design variable x_i.

Combining eq. (1) and the mathematical definition of $\boldsymbol{K}_i^1$ and $\boldsymbol{M}_i^1$, and assuming that the eigenvector $\boldsymbol{u}_i$ is normalized by $\boldsymbol{M}$, it is possible to derive the sensitivity of the objective function ω_i (eq. 5).

$$\begin{cases} \frac{d\omega_i}{dx_i} = \frac{1}{2\omega_i} \boldsymbol{u}_i^T \left(\frac{1 - x_{min}}{1 - x_{min}^p} p x_i^{p-1} \boldsymbol{K}_i^1 - \omega_i^2 \boldsymbol{M}_i^1 \right) \boldsymbol{u}_i \end{cases} \tag{5}$$

In the original bi-directional evolutionary structural optimization method introduced by Huang et al., two distinct values are assumed for the design variable(x_{min} for void elements and 1 for solid elements).

The sensitivity numbers are used in evolutionary structural optimization to represent the relative ranking of elemental sensitivities. Consequently, the sensitivity numbers α_i for solid and void elements are explicitly defined as illustrated in eq. 6 if x_{min} tends to 0. Huang et al. typically recommend using $p = 3$ in the SIMP model for the topology optimization problem; as such, this paper adheres to this choice well consolidated in the literature.

$$\alpha_i = \frac{1}{p} \frac{d\omega_i}{dx_i} = \begin{cases} \frac{1}{2\omega_i} \boldsymbol{u}_i^T \left(\boldsymbol{K}_i^1 - \frac{\omega_i^2}{p} \boldsymbol{M}_i^1 \right) \boldsymbol{u}_i \; for \; x_i = 1 \\ -\frac{\omega_i}{2p} \boldsymbol{u}_i^T \boldsymbol{M}_i^1 \boldsymbol{u}_i \; for \; x_i = x_{min} \end{cases} \tag{6}$$

However, optimization techniques frequently tend to perform poorly with local minima without filtering, making mesh dependence of their solutions inevitable. Several filtering strategies have been used to overcome this problem in the literature (Huang and Xie 2007; Sigmund and Maute 2013). The optimization problem is regularized and smoothed down with these filters, improving convergence behaviour and producing more consistent results.

Mesh-independency filters guarantee that the optimization results remain similar at various mesh resolutions. These filters improve robustness and lessen susceptibility to mesh details by smoothing the design variables or gradients.

Thus, a mesh-independency filter addresses issues related to checkerboard patterns and mesh dependency (Huang and Xie 2009). This filter involves averaging the elemental sensitivity number with its neighbouring elements using image-processing techniques.

The sensitivity numbers α_j^n at the nodes, obtained by averaging the sensitivity numbers of interconnected elements, are reconverted into elements using the filtering scheme outlined in eq. 7 where r_{ij} represents the distance between the center of the element i and the node j, M stands for the total number of nodes in the structure, and $w(r_{ij})$ represents the weight factor.

$$\widehat{\alpha}_i = \frac{\sum_{j=1}^{M} w(r_{ij}) \alpha_j^n}{\sum_{j=1}^{M} w(r_{ij})} \; where \; w(r_{ij}) = \begin{cases} r_{min} - r_{ij} \; for \; r_{ij} < r_{min} \\ 0 \; for \; r_{ij} \geq r_{min} \end{cases} \tag{7}$$

As stated by (Huang et al. 2010), incorporating historical information into the sensitivity number through averaging is an effective technique to facilitate algorithm convergence. The optimality criterion can be characterized by ensuring that the sensitivities of solid elements consistently surpass those of void elements. Thus, the update scheme for the design variables x_i consists of transitioning from 1 to x_{min} for elements with the lowest sensitivity numbers and from x_{min} to 1 for elements with the highest sensitivity numbers.

The iterative process for the modified BESO method typically initiates from a bulk design domain and systematically reduces the overall volume of the structure. This reduction is governed by an evolutionary rate Er, representing the ratio between the volume decrease and the current design volume. Simultaneously, the added volume is constrained by the maximum addition ratio Ar, defining the ratio between the maximum allowable addition and the current design volume. Often, the literature proposes an equivalent value for both Er and Ar. Once the target volume is attained, the design volume remains constant. The entire evolutionary process concludes when the solution achieves convergence, meaning a change in the investigated natural frequency lower than a prescribed tolerance (10^{-3} used in this study).

As previously stated, the method proposed by Huang et al. generally starts with a full design volume; however, this ideal condition is far from

real-life components, and the initial domain can be partially inaccessible to the optimizer. Inaccessible regions could be present due to assembly constraints (i.e., holes for threaded connections), no-design spaces (i.e., wires passing), or other design volume limitations.

The approach proposed in this manuscript aims to fill this technological gap by merging the previously described topology optimization approach with the voxelization method discussed in the following subsection. The preliminary voxelization phase is applied to a complex design domain, which is comprehensive of no-design spaces and converted into a logical 3D matrix. Thus, the optimization algorithm can be applied to any initial geometry described as an active subset of the overall bounding box of the component. The no-design spaces and holes are described as passive discrete elements and are not considered during the optimization. This way, the Huang approach can be of general purpose and not limited to simple academic geometries.

2.2 Voxel-based graphic visualization

In contrast to conventional 3D representation techniques, voxel-based modeling excels in handling larger datasets, preserving intricate details within the interiors of 3D models, and expediting geometric manipulations and operations such as boolean operations and rotations. Voxelization is seldom prone to failures due to its straightforward unit cell topology, especially compared to more intricate discretization methods (Lerebours et al. 2019).

Many voxelization algorithms involve overlaying a 3D grid onto the 3D model, enabling the determination of whether the actual object occupies a single unit cell (voxel) or not. Each voxel is assigned a binary value, contributing to the population of a 3D logical matrix: 0 if the unit cell lies outside the 3D model and 1 otherwise (Fig. 1).

In this research, to apply voxelization, the algorithm requires the designer to provide the 3D model of the object to optimize, and the algorithm automatically determines the bounding box dimensions of the model. The user should possess the 3D model in the form of a Standard Triangulated Language (STL) file (Qu and Stucker 2005) and should specify the voxel resolution d, which is the size of the edges (or square in the case of 2D voxelization) of the cubes used for discretization. This choice directly influences the spatial grid of the voxels S_{x_i}. Once the voxel grid is known, the algorithm initializes a logical matrix with all null values. In the next step, the algorithm automatically performs ray tracing in the three principal directions (x, y and z). It consolidates the results from each dimension to identify which elements of the logical matrix should be activated (Fig. 2).

In particular, the voxelization process for each triangle in the STL file involves the following sequential steps:

1. Identify the edges of the triangle.
2. Calculate the vertex opposite to the chosen edge.
3. Determine the ray associated with the selected edge.
4. Verify whether the ray aligns with the same side of the chosen edge.
5. The ray intersects the facet if the affirmation holds true for all triangle edges. Consequently, the corresponding matrix element should be activated.

2.3 Routine for the structural connectivity check

When aiming for low-volume fractions, conventional frequency optimization algorithms may yield a partially or unconnected component that is not manufacturable. The proposed method incorporates a *connectivity check* routine that monitors the complete connectivity of the optimized structure at each iteration, employing the bwconncomp function in MATLAB. This function identifies and quantifies the connected components in a provided binary matrix. The output structure returns the total count of connected components, Regions Of Interest (ROIs), and the pixel indices assigned to each component. When considering the bwconncomp function, the default connectivity value is set to 8 for two dimensions and to 26 for three-dimensional matrices (Fig. 3c). For this research, the default value (Fig. 3c) is used, but in the future, other types of connectivity will be investigated to understand how this value may affect the resulting structure.

The algorithm performs the connectivity analysis once the new design (in terms of a logical matrix) is constructed at each iteration of the optimization routine based on calculating, filtering, and averaging

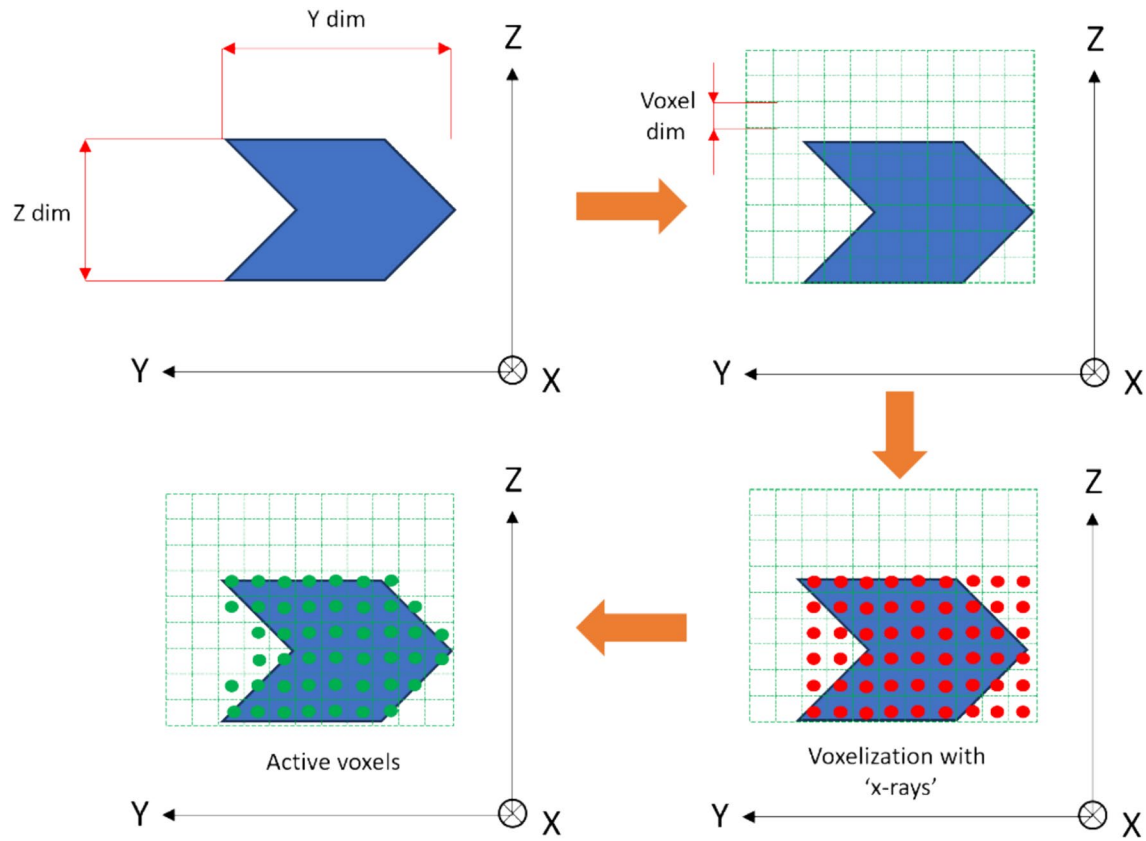

Fig. 1 Ray tracing voxelization methodology along 'X' applied on a sample shape

the sensitivity numbers of each element. The logical matrix is given as input to the connectivity function. If more than one ROI is detected, the ID of the active element closest to the main structure is selected $\widetilde{x_i}$ (active element highlighted in red in Fig. 4): this means that a subset of active elements is not connected to the main structure.

The main structure is defined as the ROI with the highest number of active voxels assigned to each component. To find $\widetilde{x_i}$, the algorithm builds a 3D relative distance matrix, where, for each (i,j) position, the relative distance between x_i and x_j is saved.

Once $\widetilde{x_i}$ has been detected, an in-plane 3×3 logical matrix of active elements is built around $\widetilde{x_i}$ to close the gap and connect two ROIs (Fig. 5). Moreover, the algorithm flags $\widetilde{x_i}$ and all the elements belonging to the in-plane added matrix. Suppose these elements are removed by the BESO routine in future iterations and added more than twice by the *connectivity check* routine. In that case, the algorithm locks these elements' logical value to 1 and saves them into a *no-design space* array to avoid a scattering behaviour of the optimization function.

Indeed, for the scope of this research, the implemented algorithm embeds a *no-design-space* array. This array contains all the discrete elements that should be fixed to the initial logical value and defines a volume subset that will not be considered in the optimization routine. This array is automatically compiled with the IDs of the elements where the boundary conditions are applied (fixed nodes) and where the eventually added masses are located. Moreover, the array mentioned above can be populated by elements deleted by the BESO routine more than twice and re-activated by the *connectivity check* routine (for this reason, a flag that counts the number of times an element is deleted is introduced), especially in the regions repopulated by the connectivity routine.

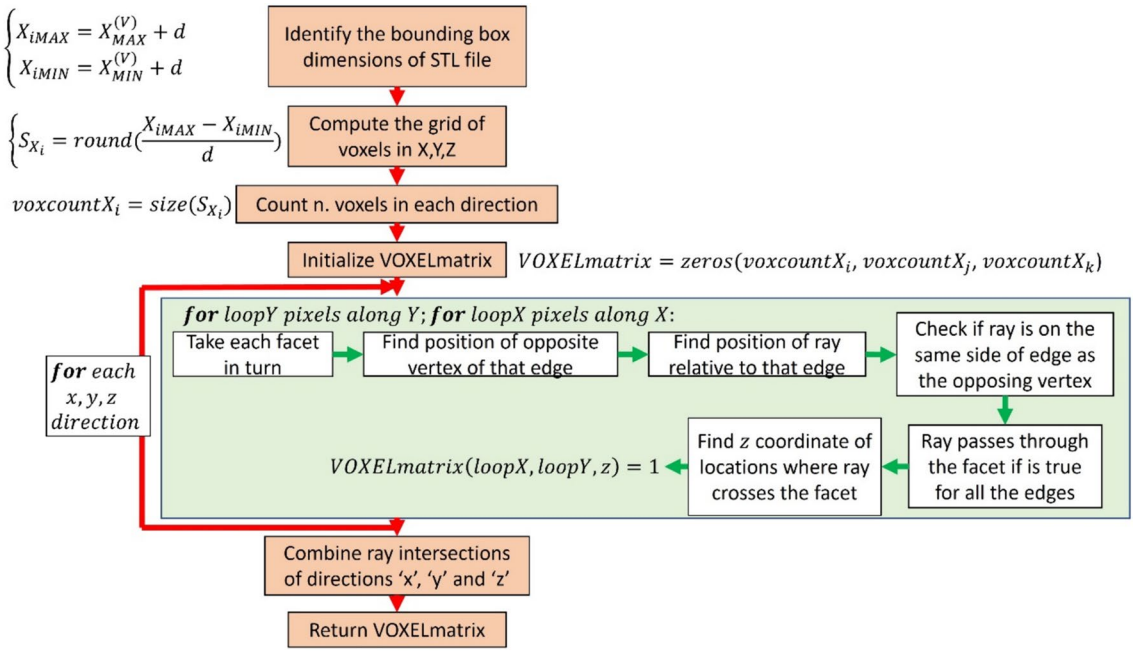

Fig. 2 Graphic flowchart of the ray tracing voxelization methodology [adapted from (Bacciaglia et al. 2022)]

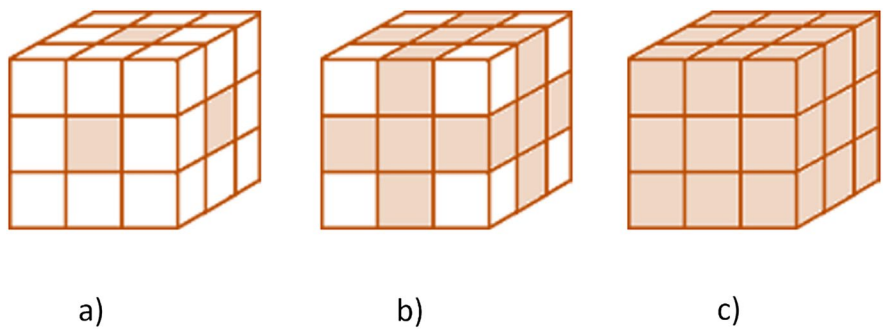

Fig. 3 Three-dimensional connectivities provided by bwconncomp Matlab function. **a** Pixels are connected if their faces touch and are connected along the three principal directions (connection with 6 elements), **b** Pixels are connected if their faces or edges touch and are connected along the three principal directions and a combination of two of them (connection with 18 elements), **c** Pixels are connected if their faces, edges, or corners touch, and are connected along the three principal directions and a combination of two of them and a combination of three directions (connection with 26 elements)

Once the *connectivity check* routine modifies the new design, the global mass and stiffness matrices are recomputed due to the topology modification, and the convergence status is checked. If convergence is still not satisfied because of $V > V_f$ (where V is the actual volume fraction, and V_f is the required final volume fraction) or because the solution is not stationary, the evolutionary frequency optimization performs another iteration, as explained in the following Section, where the entire optimization methodology is analyzed in detail.

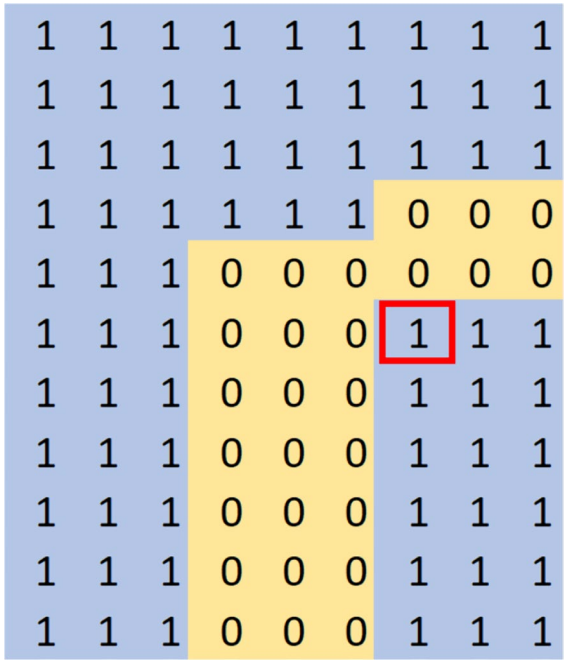

Fig. 4 Example of a 2D logical matrix with two disconnected ROIs (in light blue); $\tilde{x}_i$ has been highlighted in red

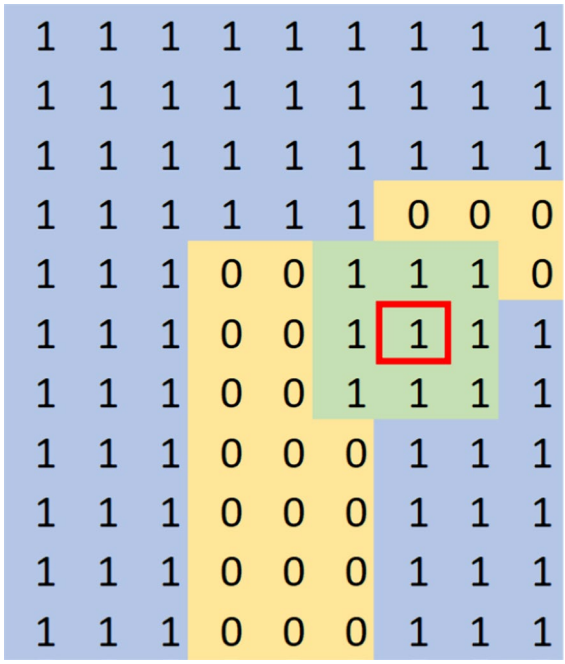

Fig. 5 The connectivity check routine builds an active 3x3 matrix (in light green) around $\tilde{x}_i$ to satisfy the connectivity of the structure

3 Numerical implementation

The flow chart in Fig. 6 illustrates the step-by-step process of the proposed voxel-based evolutionary topology optimization method. The flowchart contains some innovative steps compared to the Huang et al. approach, highlighted with a green square. This Section will mainly focus on describing these additional steps, while the reader can refer to (Huang et al. 2010) for the standard BESO procedure for frequency optimization. The methodology described in Fig. 6 has been implemented in the MATLAB environment, developing a GUI embedding all the features necessary to run an optimization.

After defining the bounding box dimensions, the material properties, and the voxelization resolution, the user is asked to import the 3D model of the design domain as an STL file format (i.e. red 3D model visible in Fig. 7a). This way, the design domain could be of whatever complex shape (such as the triangular prism of Fig. 7a) and is not restricted to a whole parallelepiped design domain, as in Huang et al., with limited applicability in a real-life scenario.

Then, the 3D design domain is voxelized with the method described in Section 2.2 and saved in the memory (Fig. 7b); for the remainder of the article, the resulting logical 3D matrix, visible both in terms of memory content and 3D shape in Fig. 7b, will be referred to as the *initial logical design domain*.

The *initial logical design domain* refers to the 3D logical matrix of the design domain (of whatever shape) that has been voxelized. Indeed, the voxelization is always applied to a parallelepiped bounding box (visible in grey in Fig. 7a) and subdivided into small hexahedral elements in the following. Thus, the design domain does not match the bounding box dimensions. The regions that do not belong to the design volume but are part of the bounding box will be automatically deactivated (value 0) during the voxelization process.

The derived 3D logical matrix is called the *initial logical design domain* since it describes the design domain logically (matrix filled with 0 and 1) before the optimization procedure starts.

After running the MATLAB code and importing the design volume, the user is asked to graphically select the nodes of the voxel-based mesh where fixed point boundary constraints are applied through the GUI coded in MATLAB developed by the authors

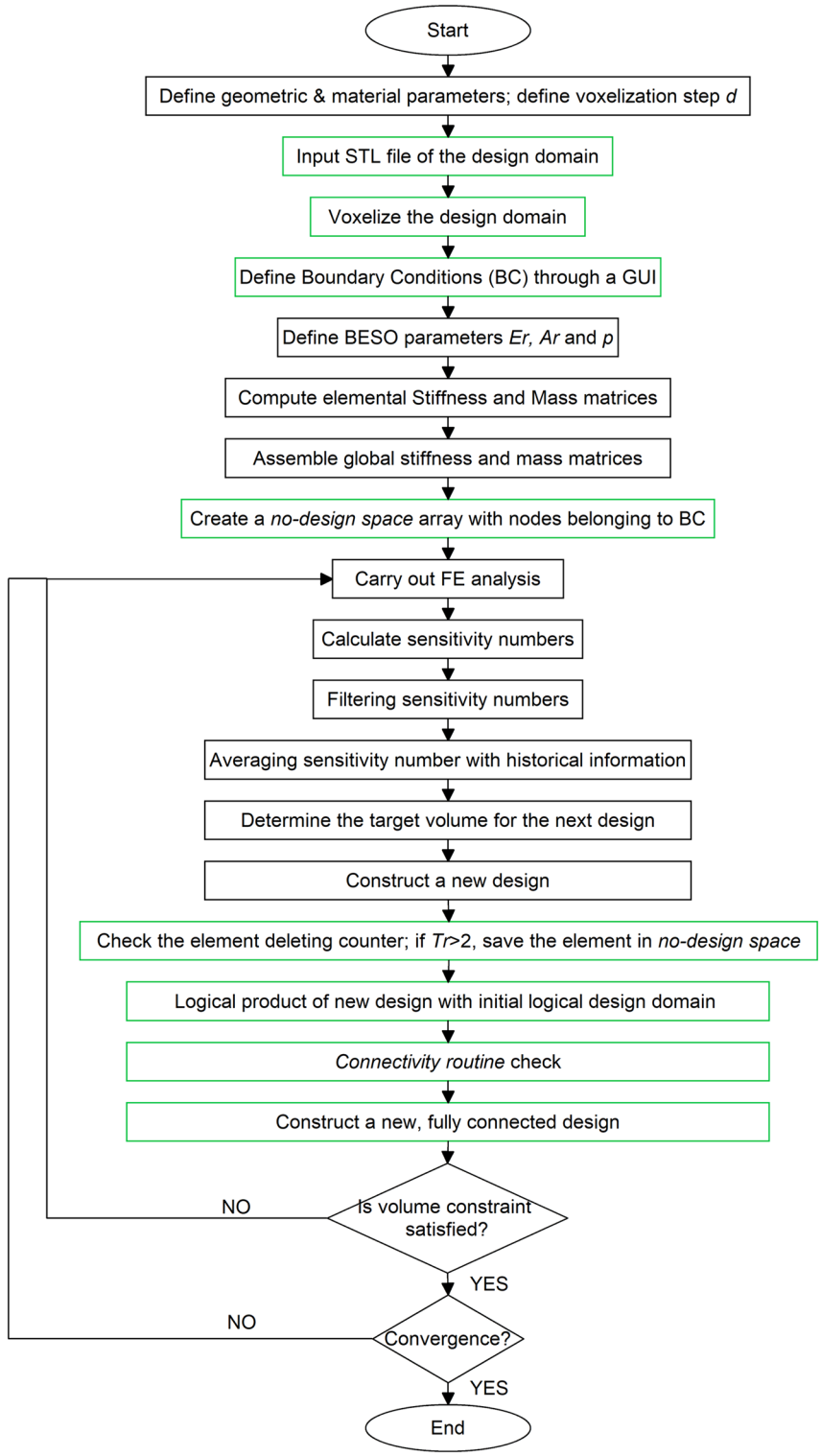

Fig. 6 Flowchart of the proposed voxel-based BESO procedure with connectivity check

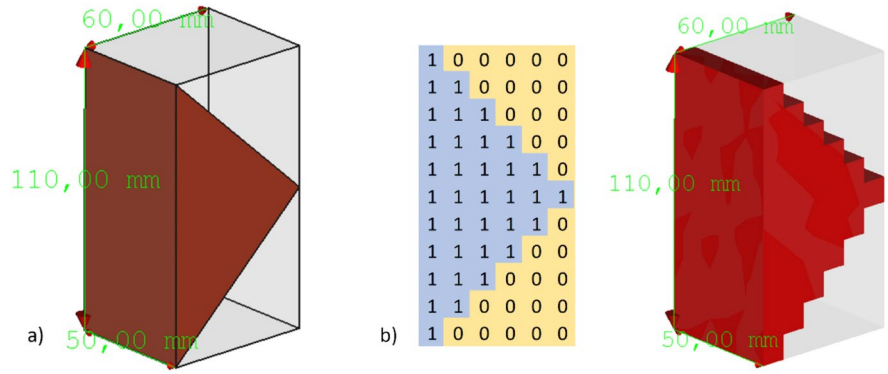

Fig. 7 **a** A 3D digital model representing the design domain of the optimization problem is shown in red with a bounding box represented in grey, **b** the design domain is voxelized, and a 3D voxel-based representation is obtained

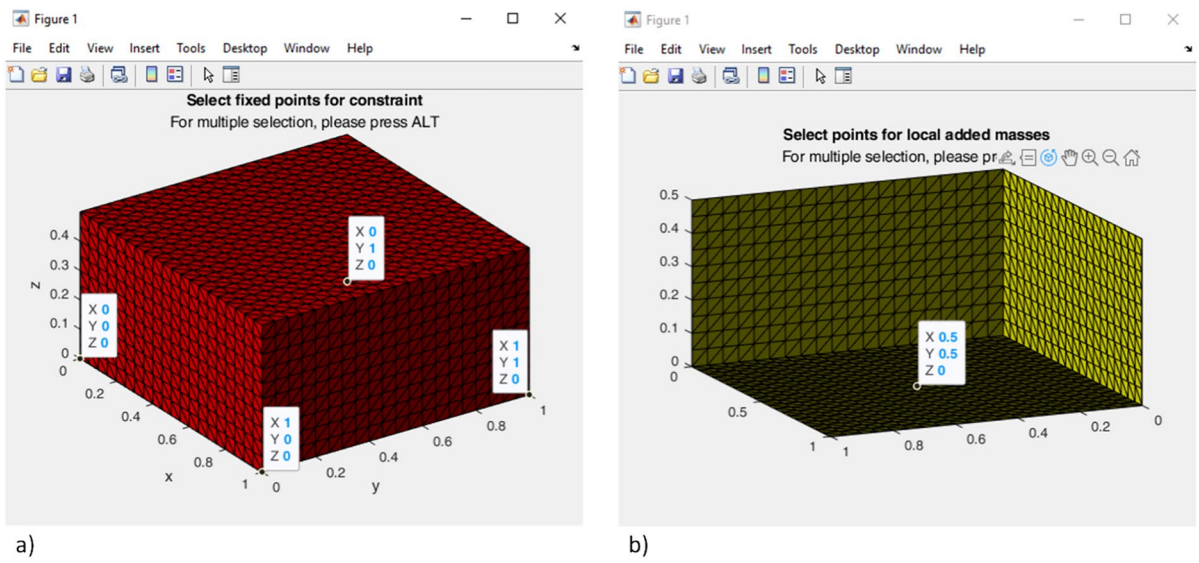

Fig. 8 MATLAB GUI developed by authors to select a) the fixed points and b) concentrated local added masses; here, the 3D case study implemented by Huang et al. is chosen as a reference with a four-supported cube design domain with a locally added mass at the center of the bottom face

(Fig. 8a). Moreover, the user can optionally place concentrated added masses to the design domain by selecting one or more nodes of the voxel-based mesh (Fig. 8b). In this way, the methodology can be applied to several design problems close to industrial real-life applications, without limiting itself to academic case studies.

The following steps involve defining some BESO parameters and evaluating the initial design domain's elemental and global stiffness and mass matrices, similar to Huang's approach. Afterwards, the new method described in the present paper differs in defining a no-design-space array, as mentioned in Section 2.3. This array includes the element IDs where the boundary constraints are applied, including the position of the local added masses. These elements will always be active during the entire optimization process to satisfy the operating conditions of industrial components and obtain a genuinely manufacturable and usable component.

The user can easily define the fixed points IDs and position of concentrated masses by clicking on the GUI shown in Fig. 8 on the desired mesh points; the algorithm automatically saves the coordinates of these points.

Consequently, the iterative BESO approach initiates from the original design, saved inside the *initial logical design domain,* and progressively

reduces the overall structure volume with an evolutionary rate (Er) that specifies the proportion between the volume decrease and the current design volume at the iteration i, V_i (eq. 8).

$$V_i = V_{i-1}(1 - Er) \tag{8}$$

Moreover, the definition of the initial volume (V_1) changes compared to Huang et al.. Indeed, the 3D initial logical matrix describes the parallelepiped bounding box that comprehends even void voxels not belonging to the initial component. Thus, V_1 can be defined as the sum of the true values of the *initial logical design domain* matrix. Simultaneously, the additional volume is constrained by the maximum addition ratio (Ar), which determines the proportion between the maximum permissible addition volume and the current design volume.

As a new step before the convergence check, the algorithm monitors if a particular element has been deleted and added more than a certain number of times at each iteration. In the following, this value will be called the *threshold value* (Tr). If this check is true, then the ID of the element is saved inside the *no-design-space* array, and the logical value of that element will be fixed to 1. This step has been added to force the algorithm to accept true values of voxels added by the *connectivity check* routine (described in Section 2.3) and to avoid a rebounding effect between two similar designs where a particular element is added and removed several times. From a coding point of view, a numerical flag is added for each element, and if the element is deleted, the flag is increased by a step.

$Tr = 2$ has been selected after some trials in this paper: the 3D case study proposed by (Huang et al. 2010) has been taken as a reference, and a unitary step in each simulation systematically increased the threshold value. This analysis makes it possible to understand the best threshold value, considering the output frequency that should be as close as possible to the reference value from the literature, by paying attention to the number of iterations and simulation time (using the same workstation and test conditions). These simulations consistently yielded the same resulting structure (Fig. 9) and natural frequency values. In Table 1, the number of iterations and the time required to achieve convergence are collected, showing significant variations among the different simulations. The first row contains the simulation information regarding the methodology proposed by (Huang et al. 2010), considered a benchmark.

Additionally, at each iteration of the optimization process, the 3D matrix describing the new design is logically multiplied by the *initial logical design domain* matrix (Fig. 10). This mathematical operation describes the geometrical and logical intersection operation between the *initial logical design domain*

Table 1 Comparison of threshold values for the element deleting counter; the first row contains the simulation information regarding the methodology proposed by (Huang et al. 2010), considered a benchmark. The relative simulation time and first natural frequencies are computed relative to the benchmark simulation in the first row

Threshold value	Iterations	Relative Simulation Time	Relative 1st natural frequency
None (Huang)	79	1	1
1	77	0.97	1.02
2	74	0.94	1.03
3	94	1.21	0.99
4	108	1.52	1.01

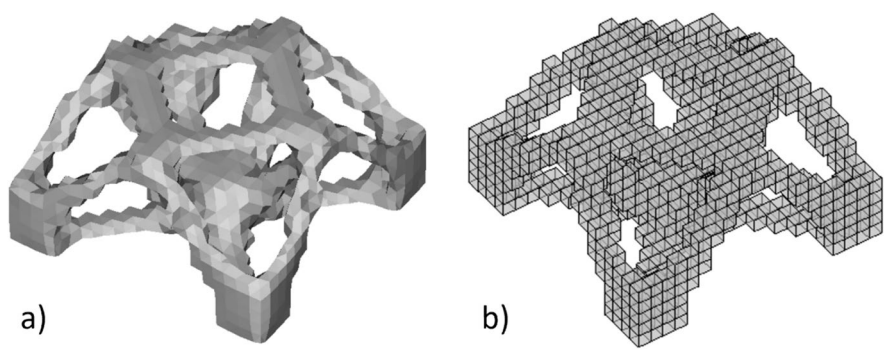

Fig. 9 Replication of results obtained in Huang et al. Optimal design for the 3D cube. **a** CAD model and **b** FE model

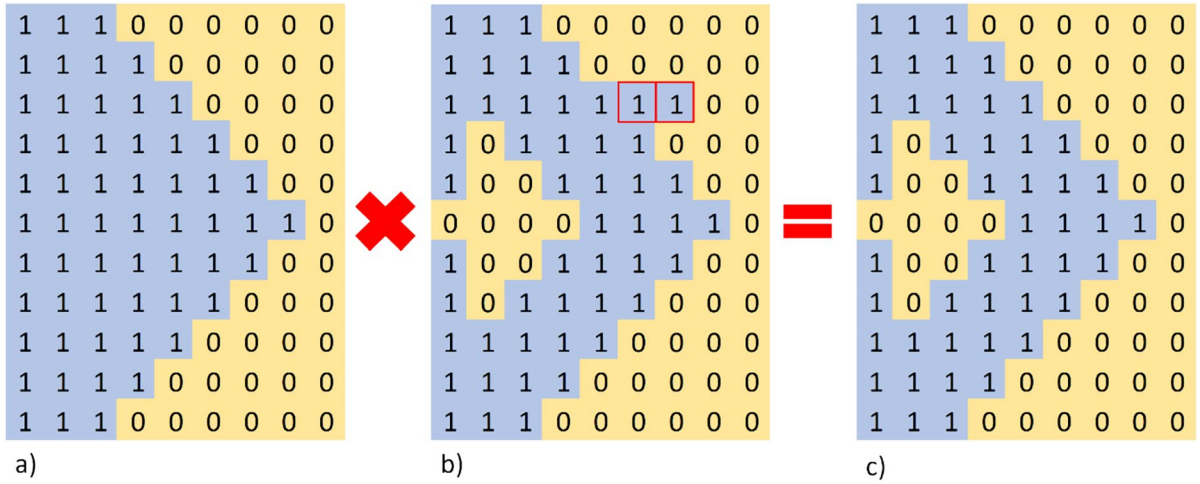

Fig. 10 The logical product of the initial logical design domain **a** and the design at the i-th iteration of the process **b,** where some active elements added by the BESO approach and highlighted in red are outside the design domain, resulting in a new structure conformal to the design domain constraints **c**

and the optimized design at the i-th iteration. This way, the algorithm's behaviour is controlled, and elements with a value of 1 outside the design volume are deactivated (Fig. 10c).

Before the algorithm controls the volume fraction of the new design and the convergence criterium, the last innovative step of the methodology described in this paper involves the *connectivity check* routine, which has already been deeply analyzed in Section 2.3. This way, the algorithm avoids new partially connected designs that are unfeasible from a manufacturing point of view. The reader is referred to Section 2.3 for further details on the routine mentioned here.

As the last step of the iterative numerical implementation visible in Fig. 6, the design volume remains constant after reaching the specified volume fraction. The evolutionary process concludes when the solution converges, meaning the natural frequency changes in two subsequent iterations are below the prescribed tolerance.

3.1 Effect of Algorithm Settings on Optimal Topologies

This subsection discusses how the optimal geometry is affected by the input settings of the proposed approach.

The Voxel-based evolutionary topological optimization requires as inputs the following parameters:

- Material penalization factor p (with values $p \geq 3$ (Bendsøe and Sigmund 2011));
- Evolution rate Er ($Er = 2\%$ proposed by Huang and Xie 2009);

Regarding the mesh resolution, which corresponds to the voxel resolution for the proposed approach, there is no critical effect on the resulting structure thanks to the mesh independence filter. A finer mesh will implicate a smoother and more accurate geometry but with higher computational effort and time required to run the simulation. Due to limited computational resources, the authors decided to fix the mesh resolution. Lastly, the filter radius dimension is highly influenced by the mesh resolution. Thus, once the mesh dimension has been fixed, it is also straightforward to freeze the filter radius value.

The authors modified the material penalization factor and the evolution rate values to investigate how the input settings affect the resulting structure. The results are visible in Table 2.

Table 2 demonstrates that the configuration with $p = 5$ and $Er = 2\%$ may create some instabilities during the optimization process (visible in the frequency plot versus the algorithm iterations).

Table 2 The Effect of Algorithm Settings on the resulting structure. The (Huang et al. 2010) 3D case study has been used but with a target final volume of 40% of the allowable domain to speed up the simulations

Configuration	Geometry	Frequency
$p = 3;$ $Er = 2\%;$	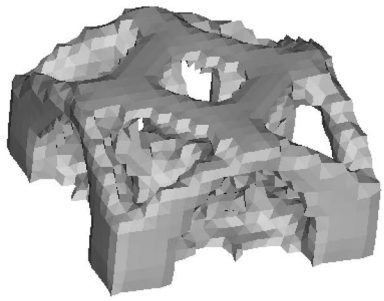	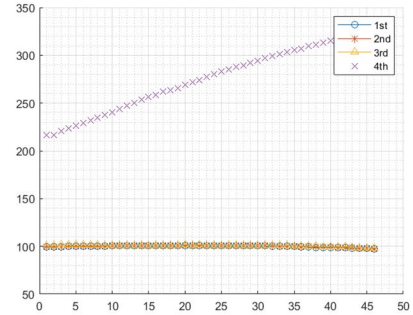
$p = 3;$ $Er = 4\%;$	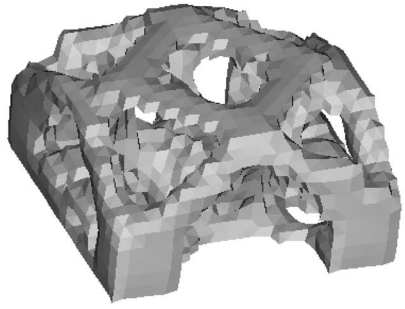	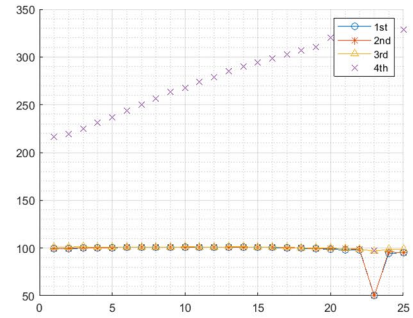
$p = 5;$ $Er = 4\%;$	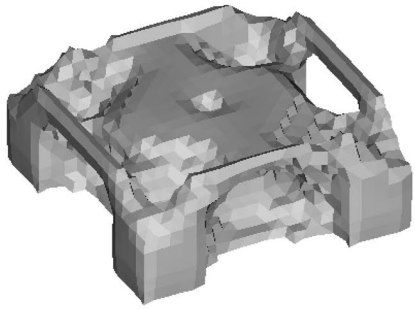	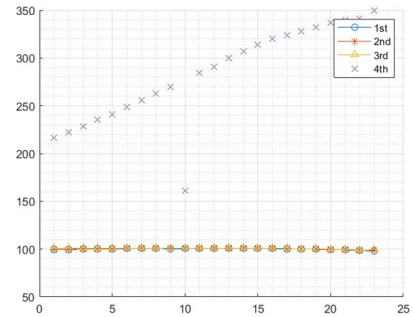
$p = 5;$ $Er = 2\%;$	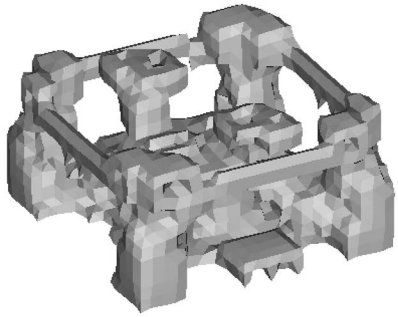	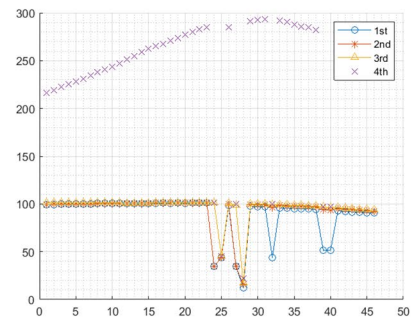

Overall, $p = 5$ provides a too-aggressive material penalization with a resulting structure quite different if compared with the literature (Huang et al. 2010). Thus, a value of $p = 3$ is more conservative and well fits the specific requirements of the proposed algorithm.

Focusing on the evolution rate, the increase from 2% up to 4% leads to a lower number of iterations required to reach the convergence (25 versus 45), visible in the frequency plots in the third column of Table 2. However, the resulting geometry shows regions where the material has been removed more aggressively (shown in red in Fig. 11) and regions where the material has been incorrectly added (shown in green in Fig. 11). This result demonstrates one more time that the value $Er = 2\%$, in accordance with the literature, should be used.

After this brief sensitivity analysis of input parameters, the values proposed in the literature will be used in the following section, where a case study representative of an actual application is simulated to showcase the algorithm capabilities described in this section.

4 Case study

A support bracket that can be mounted in satellites (Mouriaux and Berkau 2023) has been chosen to prove the capabilities of the voxel-based evolutionary topological optimization for natural frequencies. Indeed, in aerospace applications (Bacciaglia et al. 2023), components may have stringent natural frequency constraints due to environments where resonances due to cyclic loads or power spectral density can lead to failures.

The approach presented in this paper and implemented in the MATLAB environment has been applied to the selected case study. We consider the topological optimization of an inclined beam representing an antenna bracket with a rectangular cross-section fixed by clamping it at the four vertices. On the tip, a distributed mass m of 1000 kg is applied, which, for simplicity, can be conceptualized as four masses $\frac{m}{4}$ applied to the four vertices of the face (Fig. 12). The bounding box dimensions of the design space are L1 = 1 m, L2 = 1 m, and thickness L3 = 0.6 m. The material has Young's modulus $E = 200GPa$, a Poisson's ratio of $\upsilon = 0.3$, and a material density of $\rho = 7800\text{kg/m3}$. The goal is to increase the fundamental frequency of the structure as much as possible while utilizing only 50% of the total domain volume.

This shape has been set because a similar case study has been widely used to test optimization algorithms (Mouriaux and Berkau 2023).

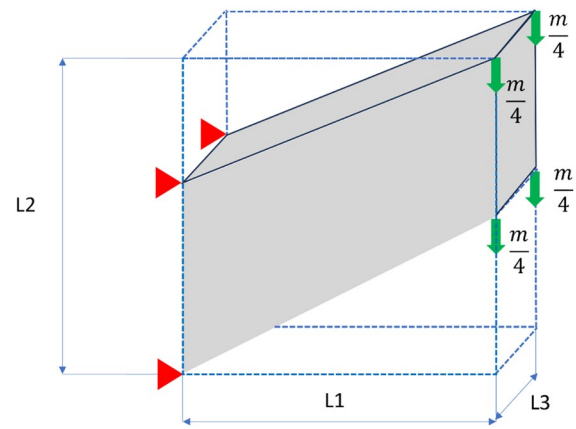

Fig. 12 Design domain of the 3D antenna bracket with four concentrate masses $\frac{m}{4} = 250$ kg at the extremities of the free end

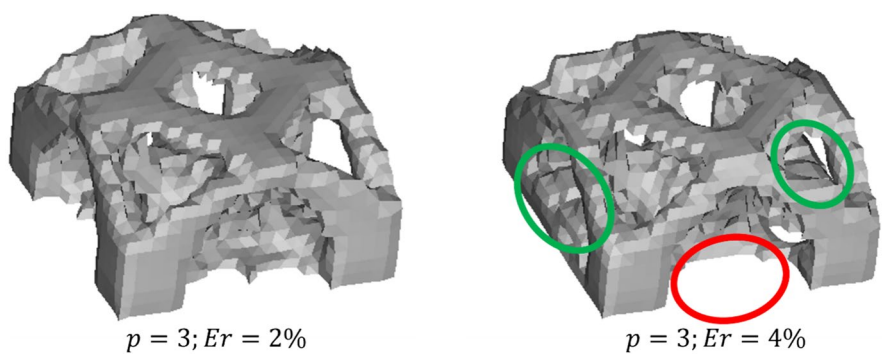

Fig. 11 Visual comparison of the resulting structure when the evolution rate Er is modified. With an increased value, the behaviour of the optimization algorithm is quite aggressive, with the optimized topology far from the benchmark

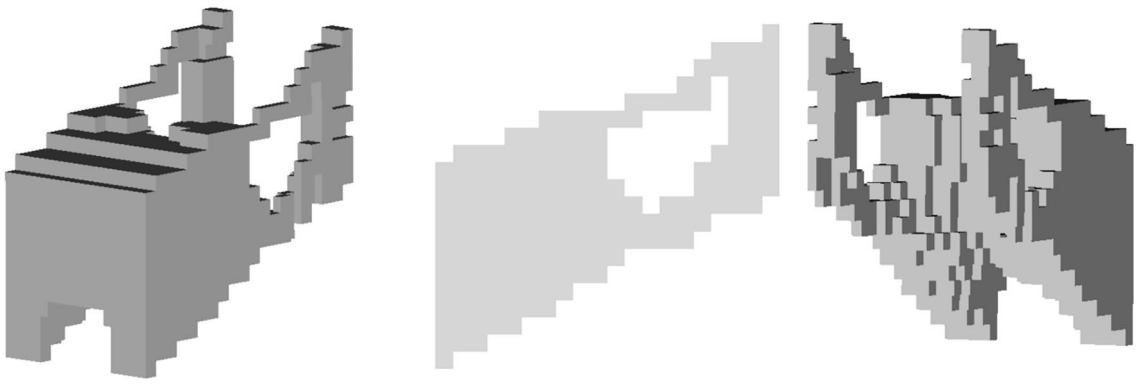

Fig. 13 Optimal design for the 3D antenna bracket from different views

Table 3 Results of the bracket optimization (values are referred to a workstation with 32 GB of RAM and a 3.50 GHz Intel Zeon CPU)

Parameter	Value	Unit
Simulation time	1987	[s]
N. iterations	30	-
V_f	0.492	-
1st Natural frequency	77.5	Hz

The parallelepiped bounding box that contains the design domain shown in Fig. 11 has been divided into a 20×20×10 mesh using eight-node cubic elements. A finer mesh could have been obtained using a high-performance workstation, but a low computational case study has been selected to reproduce the results in desktop computers. The simulations herein described have been run on a PC with 32 GB RAM and 3.50 GHz Intel Zeon CPU), thus limiting the resolution of the voxelization d. The discretization step indeed affects the dimensions of the global mass and stiffness matrices, managed as sparse matrices in MATLAB, which will then be inverted during the resolution of the FE analysis.

In order to achieve a design comprising both solid and void regions, the design variables x_i are constrained to be either 1 or $x_{min} = 10^{-6}$. The additional parameters employed in BESO include an evolutionary rate Er of 2%, a maximum Addition Ratio Ar equal to 2%, a penalty factor p of 3.0, and a filter radius r_{min} of 0.075 m, according to the literature (Huang and Xie 2010).

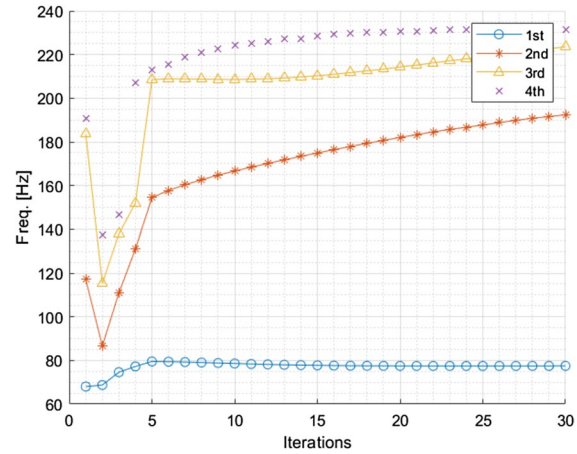

Fig. 14 Maximizing the natural frequencies of the antenna bracket with the evolution histories of the first four natural frequencies

BESO commences with the *initial logical design domain* and progressively reduces the overall volume of the structures. The ultimate optimal design is depicted in Fig. 13, resulting in ω_i= 483.8 rad/s (77.5 Hz). Table 3 collects the primary outcomes of the numerical optimization, while the corresponding evolution histories of natural frequencies are shown in Fig. 14.

The obtained 3D model, visible in Fig. 13, suffers from a high stair-step effect, typical of a voxel-based representation using discrete hexahedral elements. However, the proposed optimization methodology is compatible with standard smoothing algorithms that convert a voxel model into a manufacturable

and appealing geometry (Taubin 1995; Vollmer et al. 1999).

The *connectivity check* routine, the deleting counter function, and the logical product of initial and current logical matrices guarantee a fast computation and the feasibility of the resulting structure. Indeed, Fig. 15 visually compares the antenna bracket's resulting structure after applying Taubin's smoothing (Taubin 1995), after the topological optimization with (Fig. 15a) and without (Fig. 15b) the *connectivity check* routine, using the same settings and boundary conditions. Fig. 15c depicts the historical evolution of natural frequencies, with a sudden drop observed at iteration n. 23, likely indicating the iteration in which the structure loses its connectivity due to the continuous decrease in volume and the absence of the *connectivity check* routine.

More smoothed shapes could have been obtained by increasing the number of voxels and reducing the d parameter. Finally, to assess the quality of the natural frequency results obtained from the antenna bracket optimization, the same optimized structure was imported into commercial software and analyzed in terms of frequency. The optimized structure has a first natural frequency of 73.398 Hz. Thus, the proposed frequency optimization approach has a 5.5% error compared to the commercial software, which is taken as a benchmark. This result suggests that if the procedure is implemented in a more efficient programming language than Matlab, encouraging results could be achieved with finer meshes.

All the tests performed show that the approach we propose is adequate to handle industrial parts where the control volume has a complex shape, no design zones are mandatory to respect function requirements, and running time and code efficiency should be considered. Moreover, all the tests confirm that the methodology returns connected structures only: this is a straightforward advantage compared to the algorithms implemented in commercial software where non-connected structures are often proposed. This approach could shorten the design cycle because when a non-connected shape is obtained after a simulation, the designer must model it in CAD software by scratch, adding connection elements that could also impact natural frequencies.

5 Conclusions and future developments

Topology optimization techniques can obtain new components specifically suited to lightweight industrial applications (i.e., aerospace and automotive). Most scientific papers focus on topological optimization to minimize compliance; however, several advanced industrial applications require even constraints in the natural frequency of a part to reduce resonance problems.

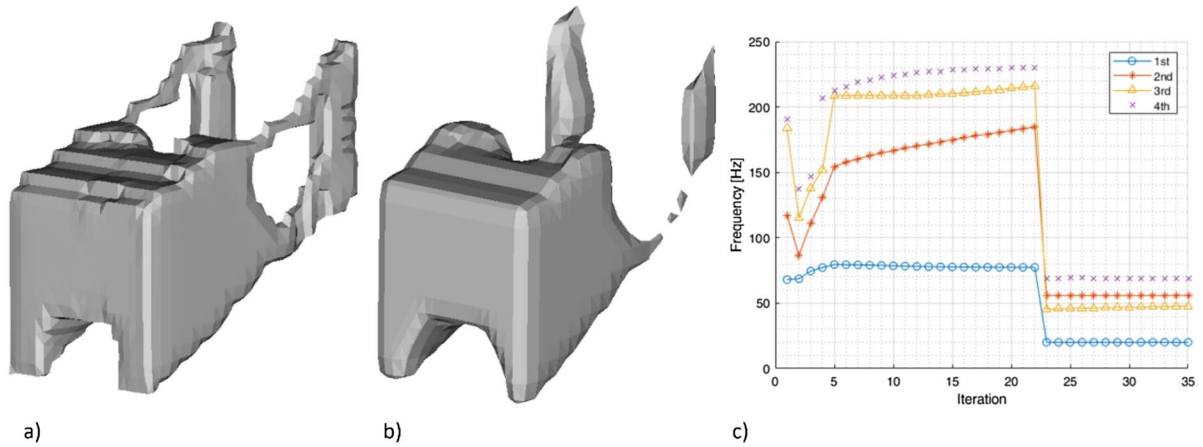

Fig. 15 Visual comparison of the antenna bracket CAD model after the frequency optimization. **a** frequency optimization with the inclusion of the connectivity check routine, **b** frequency optimization without the connectivity check routine, **c** evolution histories of the first four natural frequencies with a drop due to loss of connectivity at iteration 23 if the connectivity check routine is neglected

This paper introduces modifications to the frequency optimization algorithm developed by Huang et al. to be used for generic complex design spaces. Indeed, the proposed approach can be applied to whatever design domain whose shape may not match its bounding box (a limitation of Huang's approach we overcome). The proposed methodology includes no-design zones to respect functional requirements and structure connectivity. Indeed, the design domain may present critical regions that must be respected for manufacturing constraints: unconnected parts cannot be produced, and adding connecting elements by hand introduces a variability based on the designer's ability, which cannot be accepted in modern engineering.

The manuscript describes a methodology in which a design domain with any shape is considered, thus not limited to a bulk parallelepiped design. For this purpose, a ray tracing voxelization of the 3D model of the design domain is embedded in the optimization algorithm. Furthermore, the algorithm identifies active elements outside the design volume during the iterative process, and a logical product of the new design space with the initial logical matrix can be used to promptly deactivate undesired voxels positioned by the BESO algorithm. Moreover, an original procedure developed by the authors checks the connectivity of the new design at each iteration, avoiding shapes that are not fully connected, which are far from usable in real contexts and cannot be manufactured.

A case study dealing with an antenna bracket is included in the paper to validate and demonstrate the efficiency of the proposed method for addressing frequency optimization problems. The natural frequency value and topology consistently converge to an optimal solution, exhibiting good agreement ($\cong 5\%$ error) with results obtained through commercial optimization software packages. A qualitative and quantitative comparison of the resulting structure and historical frequency behaviour reveals that the connectivity check routine is fundamental to obtaining a fully connected structure that can be manufactured using AM techniques.

In future works, the methodology will be tested using more powerful workstations to use finer discretization and to study how the voxel resolution affects the resulting structure. Moreover, the BESO input parameters, the threshold value for the element deleting counter, and the final volume fraction should be further investigated to study how these parameters may affect the final result. Multi-objective topology optimizations could be carried out to allow complex design settings where frequency, manufacturing constraints (i.e., symmetry or layer areas), and stress are considered simultaneously.

Despite the current limitations, the voxel-based evolutionary topological optimization for natural frequencies method we developed shows high potential. It deserves further investigation based on the outcome of the present study.

Acknowledgement This study was carried out within the MOST – Sustainable Mobility National Research Center and received funding from the European Union Next-GenerationEU (PIANO NAZIONALE DI RIPRESA E RESILIENZA (PNRR) – MISSIONE 4 COMPONENTE 2, INVESTIMENTO 1.4 – D.D. 1033 17/06/2022, CN00000023). This manuscript reflects only the authors' views and opinions; neither the European Union nor the European Commission can be considered responsible for them.

Funding Open access funding provided by Alma Mater Studiorum - Università di Bologna within the CRUI-CARE Agreement.

Declarations

Conflict of interest On behalf of all authors, the corresponding author states that there is no conflict of interest.

Replication of the results All the information required to replicate the results found in Sects. 3–4 is fully disclosed in this paper. The same results will be obtained by implementing the methodology presented here. The algorithms discussed in this paper are implemented in MATLAB by the authors and can be shared by contacting the corresponding author under reasonable request.

References

Abdulhameed, O., Al-Ahmari, A., Ameen, W., Mian, S.H.: Additive manufacturing: Challenges, trends, and applications. Adv. Mech. Eng. **11**, 1–27 (2019). https://doi.org/10.1177/1687814018822880

Andreassen, E., Clausen, A., Schevenels, M., Lazarov, B.S., Sigmund, O.: Efficient topology optimization in MATLAB using 88 lines of code. Struct. Multidisc. Optim. **43**, 1–16 (2011). https://doi.org/10.1007/s00158-010-0594-7

Bacciaglia, A., Ceruti, A., Ciccone, F., Liverani, A.: Topology optimization for thin-walled structures with distributed loads. In: Gerbino, S., Lanzotti, A., Martorelli, M., Mirálbes Buil, R., Rizzi, C., Roucoules, L. (eds.) Advances on Mechanics, Design Engineering and Manufacturing IV, pp. 1042–1054. Springer International Publishing, Cham (2023)

Bacciaglia, A., Ceruti, A., Liverani, A.: A 3D voxel-based approach for fast aerodynamic analyses in conceptual design phases. CADA. **19**, 1236–1254 (2022). https://doi.org/10.14733/cadaps.2022.1236-1254

Bendsøe, M.P., Sigmund, O.: Topology optimization: theory, methods, and applications. Springer, Berlin (2011)

Cohen-Or, D., Kaufman, A.: 3D line voxelization and connectivity control. IEEE Comput. Grap. Appl. **17**, 80–87 (1997). https://doi.org/10.1109/38.626973

Deng, Z., Liang, Y., Cheng, G.: Discrete variable topology optimization for maximizing single/multiple natural frequencies and frequency gaps considering the topological constraint. Num. Meth Eng. **125**, e7449 (2024). https://doi.org/10.1002/nme.7449

Ferrari, F., Sigmund, O.: A new generation 99 line Matlab code for compliance topology optimization and its extension to 3D. Struct. Multidisc. Optim. **62**, 2211–2228 (2020). https://doi.org/10.1007/s00158-020-02629-w

Freddi, M., Ferretti, P., Alessandri, G., Liverani, A.: Reverse engineering of a racing motorbike connecting rod. Inventions. **8**, 23 (2023). https://doi.org/10.3390/inventions8010023

Ghasemi, H., Brighenti, R., Zhuang, X., Muthu, J., Rabczuk, T.: Optimal fiber content and distribution in fiber-reinforced solids using a reliability and NURBS based sequential optimization approach. Struct. Multidisc. Optim. **51**, 99–112 (2015). https://doi.org/10.1007/s00158-014-1114-y

Ghasemi, H., Park, H.S., Rabczuk, T.: A multi-material level set-based topology optimization of flexoelectric composites. Comput. Methods App. Mech. Eng. **332**, 47–62 (2018). https://doi.org/10.1016/j.cma.2017.12.005

Han, Y., Xu, B., Liu, Y.: An efficient 137-line MATLAB code for geometrically nonlinear topology optimization using bi-directional evolutionary structural optimization method. Struct. Multidisc. Optim. **63**, 2571–2588 (2021). https://doi.org/10.1007/s00158-020-02816-9

Huang, X., Xie, Y.M.: Convergent and mesh-independent solutions for the bi-directional evolutionary structural optimization method. Finite. Elements. Anal. Des. **43**, 1039–1049 (2007). https://doi.org/10.1016/j.finel.2007.06.006

Huang, X., Xie, Y.M.: Bi-directional evolutionary topology optimization of continuum structures with one or multiple materials. Comput. Mech. **43**, 393–401 (2009). https://doi.org/10.1007/s00466-008-0312-0

Huang, X., Xie, Y.M.: Evolutionary Topology Optimization of Continuum Structures: Methods and Applications. Wiley, Hoboken (2010)

Huang, X., Zuo, Z.H., Xie, Y.M.: Evolutionary topological optimization of vibrating continuum structures for natural frequencies. Comput. Struct. **88**, 357–364 (2010). https://doi.org/10.1016/j.compstruc.2009.11.011

Jense, G.J.: Voxel-based methods for CAD. Comput. Aided Des. **21**, 528–533 (1989). https://doi.org/10.1016/0010-4485(89)90061-4

Langley, R.S., Bardell, N.S.: A review of current analysis capabilities applicable to the high frequency vibration prediction of aerospace structures. Aeronaut. j. **102**, 287–297 (1998). https://doi.org/10.1017/S0001924000065325

Lerebours, A., Marin, F., Bouvier, S., Egles, C., Masquelet, A.-C., Rassineux, A.: A voxel-based method for designing a numerical biomechanical model patient-specific with an anatomical functional approach adapted to additive manufacturing. Comput. Methods. Biomech. Biomed. Eng. **22**, 304–312 (2019). https://doi.org/10.1080/10255842.2018.1552684

Liang, Y., Sun, K., Cheng, G.: Discrete variable topology optimization for compliant mechanism design via Sequential Approximate Integer Programming with Trust Region (SAIP-TR). Struct. Multidisc. Optim. **62**, 2851–2879 (2020). https://doi.org/10.1007/s00158-020-02693-2

Liang, Y., Yan, X., Cheng, G.: Explicit control of 2D and 3D structural complexity by discrete variable topology optimization method. Comput. Methods. Appl. Mech. Eng. **389**, 114302 (2022). https://doi.org/10.1016/j.cma.2021.114302

Mouriaux, F., Berkau, A.: Antenna Bracket for RUAG's Sentinel Satellite, https://www.eos.info/en/innovations/all-3d-printing-applications/aerospace/aerospace-case-studies/ruag-aerospace-3d-printed-satellite-components

Murr, L.E.: Frontiers of 3D printing/additive manufacturing: from human organs to aircraft fabrication†. J. Mat. Sci. Technol. **32**, 987–995 (2016). https://doi.org/10.1016/j.jmst.2016.08.011

Noguchi, Y., Yamada, T.: Topology optimization of acoustic metasurfaces by using a two-scale homogenization method. Appl. Math. Modelling. **98**, 465–497 (2021). https://doi.org/10.1016/j.apm.2021.05.005

Oktay, E., Akay, H.U., Sehitoglu, O.T.: Three-dimensional structural topology optimization of aerial vehicles under aerodynamic loads. Comput. Fluids. **92**, 225–232 (2014). https://doi.org/10.1016/j.compfluid.2013.11.018

Pedersen, N.L.: Maximization of eigenvalues using topology optimization. Struct. Multidisc. Optim. **20**, 2–11 (2000). https://doi.org/10.1007/s001580050130

Qatu, M.S., Abdelhamid, M.K., Pang, J., Sheng, G.: Overview of automotive noise and vibration. IJVNV. **5**, 1 (2009). https://doi.org/10.1504/IJVNV.2009.029187

Qu, X., Stucker, B.: Circular hole recognition for STL-based toolpath generation. Rapid. Prototyp. J. **11**, 132–139 (2005). https://doi.org/10.1108/13552540510601255

Rietz, A.: Sufficiency of a finite exponent in SIMP (power law) methods. Struct. Multidisc. Optim. **21**, 159–163 (2001). https://doi.org/10.1007/s001580050180

Rozvany, G.I.N.: A critical review of established methods of structural topology optimization. Struct. Multidisc. Optim. **37**, 217–237 (2009). https://doi.org/10.1007/s00158-007-0217-0

Sigmund, O., Maute, K.: Topology optimization approaches: a comparative review. Struct. Multidisc. Optim. **48**, 1031–1055 (2013). https://doi.org/10.1007/s00158-013-0978-6

Smit, T., Aage, N., Ferguson, S.J., Helgason, B.: Topology optimization using PETSc: a Python wrapper and extended functionality. Struct Multidisc Optim. **64**, 4343–4353 (2021). https://doi.org/10.1007/s00158-021-03018-7

Taubin, G.: A signal processing approach to fair surface design. In: Proceedings of the 22nd annual conference on Computer graphics and interactive techniques—SIGGRAPH '95. pp. 351–358. ACM Press, Not Known (1995)

Torigaki, T., Fujitani, K.: Power of a voxel approach to structural analysis and topology-shape optimization in automobile industries. Jpn. J. Indust. Appl. Math. **17**, 129–147 (2000). https://doi.org/10.1007/BF03167341

Vollmer, J., Mencl, R., Muller, H.: Improved laplacian smoothing of noisy surface meshes. Comput. Gr. Forum. **18**, 131–138 (1999). https://doi.org/10.1111/1467-8659.00334

Wu, Z., Fan, F., Xiao, R., Yu, L.: The substructuring-based topology optimization for maximizing the first eigenvalue of hierarchical lattice structure. Numer. Method. Eng. **121**, 2964–2978 (2020). https://doi.org/10.1002/nme.6342

Xia, L., Xia, Q., Huang, X., Xie, Y.M.: Bi-directional evolutionary structural optimization on advanced structures and materials: a comprehensive review. Arch. Computat. Methods. Eng. **25**, 437–478 (2018). https://doi.org/10.1007/s11831-016-9203-2

Xie, Y.M., Steven, G.P.: Evolutionary structural optimization for dynamic problems. Comput. Struct. **58**, 1067–1073 (1996). https://doi.org/10.1016/0045-7949(95)00235-9

Zargham, S., Ward, T.A., Ramli, R., Badruddin, I.A.: Topology optimization: a review for structural designs under vibration problems. Struct. Multidisc. Optim. **53**, 1157–1177 (2016). https://doi.org/10.1007/s00158-015-1370-5

Zhuang, C., Xiong, Z., Ding, H.: An efficient 2D/3D NURBS-based topology optimization implementation using page-wise matrix operation in MATLAB. Struct. Multidisc. Optim. **66**, 254 (2023). https://doi.org/10.1007/s00158-023-03701-x